The helical domain of GBP-1 mediates the inhibition of endothelial cell proliferation by inflammatory cytokines

Eric Guenzi, Kristin Töpolt, Emmanuelle Cornali[1,2], Clara Lubeseder-Martellato, Anita Jörg, Kathrin Matzen, Christian Zietz[3], Elisabeth Kremmer[4], Filomena Nappi[5], Martin Schwemmle[6], Christine Hohenadl[7], Giovanni Barillari[5], Erwin Tschachler[8], Paolo Monini[5], Barbara Ensoli[5] and Michael Stürzl[9]

Department of Virus-induced Vasculopathy, Institute of Molecular Virology, GSF-National Research Center for Environment and Health, Ingolstädter Landstrasse 1, D-85764 Neuherberg, [1]Department of Virus Research, Max Planck Institute for Biochemistry, D-82152 Martinsried, [3]Institute of Pathology, Ludwig Maximilians University, D-80337 Munich, [4]Institute of Molecular Immunology, GSF-National Research Center for Environment and Health, D-81377 Munich, Germany, [5]Laboratory of Virology, Retrovirus Division, Istituto Superiore di Sanità, 00161 Rome, Italy, [6]Department of Virology, Institute of Medical Microbiology and Hygiene, University of Freiburg, D-79104 Freiburg, Germany and [8]Department of Dermatology, Division of Immunology, Allergy, and Infectious Diseases, University of Vienna Medical School, 1090 Vienna, Austria

[2]Present address: Ingenium Pharmaceuticals AG, Frauenhoferstrasse 13, D-82152 Martinsried, Germany
[7]Present address: Austrian Nordic Biotherapeutics, Veterinärplatz 1, 1210 Vienna, Austria

[9]Corresponding author
e-mail: stuerzl@gsf.de

E.Guenzi, K.Töpolt, E.Cornali and C.Lubeseder-Martellato contributed equally to this work

Inflammatory cytokines (IC) activate endothelial cell adhesiveness for monocytes and inhibit endothelial cell growth. Here we report the identification of the human guanylate binding protein-1 (GBP-1) as the key and specific mediator of the anti-proliferative effect of IC on endothelial cells. GBP-1 expression was induced by IC, downregulated by angiogenic growth factors, and inversely related to cell proliferation both *in vitro* in microvascular and macrovascular endothelial cells and *in vivo* in vessel endothelial cells of Kaposi's sarcoma. Experimental modulation of GBP-1 expression demonstrated that GBP-1 mediates selectively the anti-proliferative effect of IC, without affecting endothelial cell adhesiveness for monocytes. GBP-1 anti-proliferative activity did not affect ERK-1/2 activation, occurred in the absence of apoptosis, was found to be independent of the GTPase activity and isoprenylation of the molecule, but was specifically mediated by the C-terminal helical domain of the protein. These results define GBP-1 as an important tool for dissection of the complex activity of IC on endothelial cells, and detection and specific modulation of the IC-activated non-proliferating phenotype of endothelial cells in vascular diseases.

Introduction

Activation of endothelial cells is implicated in numerous physiological and pathological processes including cell-mediated immunity and angiogenesis during development, inflammation or tumor growth (reviewed by Cines *et al.*, 1998; Carmeliet and Jain, 2000).

The activated endothelial cell phenotype represents a time- and dose-integrated response to various stimuli originating from the blood and/or from neighboring cells and tissues. Inflammatory cytokines (IC) such as interleukin-1β (IL-1β), tumor necrosis factor-α (TNF-α) and interferon-γ (IFN-γ), as well as angiogenic growth factors (AGF) such as vascular endothelial cell growth factor (VEGF) and basic fibroblast growth factor (bFGF), are the best characterized and most potent paracrine regulators of endothelial cell activity. For example, IC activate endothelial cell adhesiveness for leukocytes (Bevilacqua *et al.*, 1985; Cavender *et al.*, 1991) and are potent inhibitors of endothelial cell proliferation (Frater-Schroder *et al.*, 1987; Friesel *et al.*, 1987; Schweigerer *et al.*, 1987; Cozzolino *et al.*, 1990). In contrast, VEGF and bFGF activate endothelial cell proliferation (Folkman and Klagsbrun, 1987; Ferrara and Henzel, 1989; Keck *et al.*, 1989). VEGF, in addition, induces endothelial cell adhesiveness for leukocytes (Melder *et al.*, 1996; Detmar *et al.*, 1998), whereas bFGF inhibits the expression of adhesion molecules on endothelial cells (Griffioen *et al.*, 1996a,b).

In vivo, several of these factors are simultaneously present and active on endothelial cells. Moreover, the effect of a single factor on the endothelium may vary from tissue to tissue. For example, IC have been shown to induce angiogenesis in some *in vivo* models (Frater-Schroder *et al.*, 1987; Mahadevan *et al.*, 1989; Montrucchio *et al.*, 1994; Gerol *et al.*, 1998; Torisu *et al.*, 2000) or to inhibit angiogenesis in others (Cozzolino *et al.*, 1990; Norioka *et al.*, 1994; Yilmaz *et al.*, 1998; Fathallah-Shaykh *et al.*, 2000). In addition, according to their concentrations IC may act either as pro- or anti-angiogenic molecules in the same model systems (Fajardo *et al.*, 1992). The angiogenic effect of IC has been attributed to the recruitment of monocytes into tissues that, in turn, may release angiogenic factors (Frater-Schroder *et al.*, 1987; Fajardo *et al.*, 1992; Montrucchio *et al.*, 1994; Joseph and Isaacs, 1998) or to the induction of bFGF or VEGF expression in resident cells (Samaniego *et al.*, 1997; Torisu *et al.*, 2000). The anti-angiogenic effect of IC may be caused by their anti-proliferative activity. However,

only little is known about how IC can induce opposite effects on angiogenesis.

The aim of this study was to identify genes that mediate the anti-proliferative effect of IC on endothelial cells and that may characterize the IC-activated endothelial cell phenotype in tissues. To this goal, gene expression of endothelial cells in the presence of IC or AGF was analyzed by differential display RT–PCR (DDRT–PCR) (Liang and Pardee, 1992). Using this approach, we detected the human guanylate binding protein-1 (GBP-1), which belongs to the group of large GTP-binding proteins (Prakash *et al.*, 2000a). GBP-1 was found to be strongly induced by IC and downregulated by AGF. Detailed analyses of GBP-1 expression in cultivated microvascular and macrovascular endothelial cells and in vessel endothelial cells of Kaposi's sarcoma (KS) tissues demonstrated that GBP-1 characterizes the IC-activated non-proliferating phenotype of endothelial cells *in vitro* and *in vivo*. Additionally, we showed that GBP-1 mediates the anti-proliferative effect of IC on endothelial cells without affecting cell adhesiveness. The anti-proliferative activity of GBP-1 was found to be independent of its GTPase function, but was found to be mediated by the C-terminal helical domain of the molecule.

Results

GBP-1 expression is induced in endothelial cells in vitro by IL-1β, TNF-α and IFN-γ

Initial studies were carried out to determine the appropriate concentrations of IC (IL-1β, TNF-α, IFN-γ) or AGF (bFGF, VEGF) that clearly affected proliferation of both human macrovascular umbilical vein endothelial cells (HUVEC) and microvascular endothelial cells (MVEC). Combined application of bFGF and VEGF in concentrations of 10 ng/ml each potently activated endothelial cell proliferation of both cell types, whereas IL-1β, IFN-γ and TNF-α inhibited this AGF-induced proliferation in a dose-dependent manner (Figure 1A). In order to identify genes that may mediate the anti-proliferative effect of IC on endothelial cells and may characterize the IC-activated endothelial cell phenotype, the pattern of endothelial cell gene expression in the presence of IC or AGF was compared by DDRT–PCR in MVEC (data not shown).

The gene encoding GBP-1 was the only one of several differently expressed genes identified in the DDRT–PCR study that was upregulated by IL-1β, TNF-α or IFN-γ at both the mRNA (Figure 1B, upper panel) and protein (Figure 1B, lower panels) levels. In contrast, VEGF- or bFGF-treated or untreated cells only weakly expressed GBP-1 (Figure 1B). These results were confirmed at the single cell level by immunocytochemistry (Figure 1C).

IL-1β-induced GBP-1 mRNA expression reached the maximal level at 5 h after stimulation, remaining high for at least 24 h (Figure 1D). This induction was not secondarily mediated via induction of IFN-γ expression because it was also observed when cellular protein synthesis was abolished by cycloheximide (Figure 1E). In addition, IL-1β did not induce IFN-γ expression in HUVEC (Figure 1F).
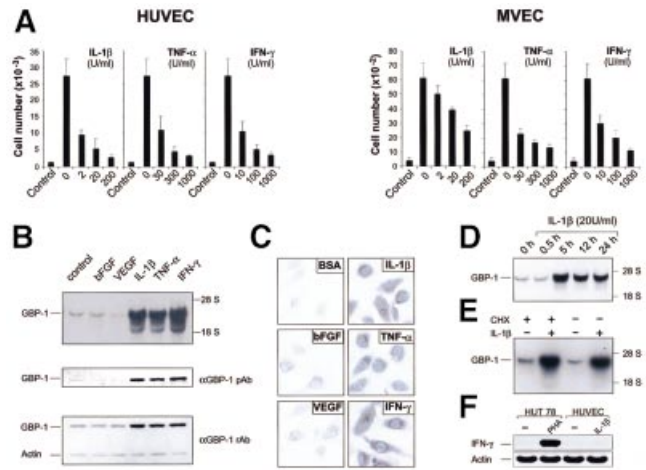

Fig. 1. Inflammatory cytokines inhibit endothelial cell proliferation and induce expression of GBP-1. (**A**) Proliferation assay with HUVEC and MVEC upon addition of AGF (VEGF and bFGF, 10 ng/ml each, except control) and increasing concentrations of IL-1β, TNF-α or INF-γ. (**B**) Northern blot (upper panel) and western blot (lower panels) analyses of GBP-1 expression in MVEC incubated with either bFGF (10 ng/ml), VEGF (10 ng/ml), IL-1β (20 U/ml), TNF-α (300 U/ml), IFN-γ (100 U/ml), or control medium for 5 h and 8 h, respectively. Polyclonal rabbit anti-GBP-1 peptide antibody (αGBP-1 pAb), polyclonal rabbit anti-GBP-1 antibody (αGBP-1 rAb), actin control (Actin). (**C**) Immunostaining for detection of GBP-1 expression in HUVEC stimulated for 8 h as described in (B). (**D**) Northern blot analyses of GBP-1 mRNA expression in MVEC after incubation for various periods of time with IL-1β; (**E**) in the presence or absence of cycloheximide (CHX, 50 μM) and IL-1β (20 U/ml, 5 h induction). (**F**) RT–PCR analysis of IFN-γ expression in HUVEC and HUT 78 lymphocytes stimulated for 5 h with IL-1β (20 U/ml) and phytohemagglutinin-L (PHA, 5 μg/ml), respectively. Actin mRNA was amplified as a control.

GBP-1 mRNA and protein expression induced by IC correlate inversely with endothelial cell proliferation in vitro

Experiments with combined IC and AGF showed that GBP-1 expression can be induced by IL-1β, TNF-α or IFN-γ in the presence of AGF either by adding the cytokines to the cells simultaneously (Figure 2A) or in AGF-pretreated cells (Figure 2C). On the other hand, IC-induced GBP-1 expression was consistently reduced by the addition of AGF, both in HUVEC and MVEC (Figure 2B). A more detailed analysis confirmed that VEGF as well as bFGF significantly reduced IL-1β-induced GBP-1 expression and that both factors together had additive inhibitory effects on GBP-1 expression at both the RNA (Figure 2D, white columns) and protein (Figure 2E, white columns) levels. Most importantly, in the presence of IC endothelial cell proliferation (Figure 2D and E, black columns) was inversely related to GBP-1 mRNA and protein expression (Figure 2D and E, white columns; compare also Figures 1A and 2A). This indicated that GBP-1 characterizes the IC-activated non-proliferating phenotype of endothelial cells *in vitro*.

GBP-1 expression correlates inversely with endothelial cell proliferation in KS in vivo

To investigate whether GBP-1 expression may define the IC-induced non-proliferating phenotype of endothelial cells *in vivo* also, double staining experiments and *in situ*

hybridization studies were performed on KS (reviewed by Ensoli *et al.*, 2001; Stürzl *et al.*, 2001). KS lesions were chosen as the *in vivo* model because they are highly vascularized (Figure 3A, black arrows) due to the production of bFGF and VEGF by the KS spindle cells, which are regarded as the tumor cells of KS [Figure 3A, white arrows (Xerri *et al.*, 1991; Ensoli *et al.*, 1994; Cornali *et al.*, 1996)]. However, lesions are also infiltrated by monocytes and lymphocytes, which locally produce IL-1β (Figure 3B, arrows), TNF-α (Figure 3C, arrows) and IFN-γ (Figure 3D, arrows), which activates endothelial cells (Stürzl *et al.*, 1995; Fiorelli *et al.*, 1998).

Tissue sections were stained simultaneously for GBP-1 protein and the monocyte specific marker CD68 (Figure 3E). GBP-1 was selectively detected in endothelial cells of vessels (Figure 3E, brown, arrow) that are sur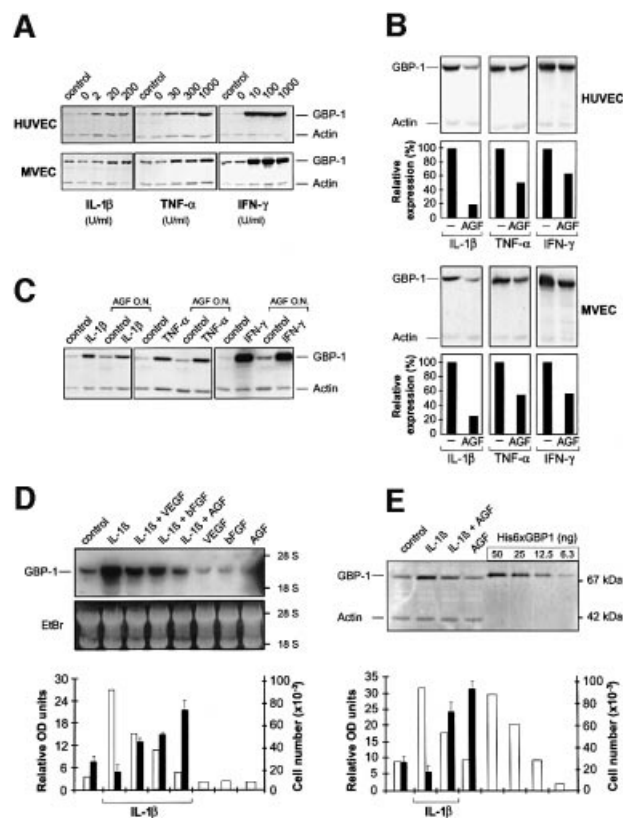rounded by numerous perivascular monocytes (Figure 3E, red). Consecutive control sections of a positive specimen with GBP-1-expressing endothelial cells (Figure 3F, arrow) did not show any staining when the primary anti-GBP-1 antibody was omitted (Figure 3G) or applied in the presence of an excess of the purified recombinant GBP-1 protein (Figure 3H).

GBP-1 expression in vessel endothelial cells was confirmed at the RNA level by *in situ* hybridization using a GBP-1-specific antisense RNA probe (Figure 3I, bright field; J, corresponding dark field, arrow). Control hybridizations with the GBP-1 sense probe did not produce any signals (Figures 3K and L).

To investigate whether GBP-1 expression may define the non-proliferating phenotype of vessel endothelial cells in KS, immunofluorescence studies for the simultaneous detection of GBP-1, the endothelial cell-associated antigen CD31 or the proliferation-associated antigen Ki67 were performed. Simultaneous expression of GBP-1 (Figure 4A, arrow; C, green) and CD31 (Figure 4B, arrow; C, red) was found only in endothelial cells of some well-differentiated vessels (Figure 4C, GBP-1/CD31 colocalization, yellow). No staining was observed in the epidermal layer overlaying KS (Figure 4C, asterisk) and in the perivascular areas containing the KS spindle cells, monocytes, lymphocytes, fibrocytes and smooth muscle cells (cellular composition of KS reviewed by Stürzl *et al.*, 2001). In contrast, in no case were GBP-1 (Figure 4D and G, arrows; F and I, green) and Ki67 (Figure 4E and H, arrows; F and I, red) found to be co-expressed in the same cell (Figure 4F and I), demonstrating that GBP-1 is not expressed in proliferating endothelial cells. Specificity of Ki67 staining was demonstrated by the positive reaction of proliferating basal cells in the epidermis (Figure 4I, asterisk).

To further prove that GBP-1 is only expressed in non-proliferating but not in proliferating endothelial cells within KS lesions, triple labeling experiments for the simultaneous detection of GBP-1, Ki67 and CD31 were performed. CD31-positive endothelial cells surrounding tumor vessels were evenly distributed in the tissue sections (Figure 4L, arrow and M, red cytoplasmic staining). In contrast, the highest numbers of GBP-1- (Figure 4J, arrow and M, green cytoplasmic staining) or Ki67- (Figure 4K, arrow and M, blue nuclear staining) positive endothelial cells were detected in different areas of the tissue section. Interestingly, areas with many Ki67-expressing endothelial cells (Figure 4M, upper part, blue arrows) revealed only few GBP-1-expressing endothelial cells, and vice versa, in areas with many GBP-1-expressing endothelial cells (Figure 4M, lower part, yellow arrows) only a few Ki67 positively stained cells were detected. The opposite local distribution of GBP-1- or Ki67-expressing endothelial cells in KS tissue sections was also observed when GBP-1 expression was investigated at the RNA level by *in situ* hybridization (data not shown).

Altogether, these data demonstrate that in KS tissues GBP-1 expression is closely associated with vessel endothelial cells and specifically detected in areas with high IC expression, whereas its expression is low or absent in proliferating endothelial cells. Since GBP-1 expression both *in vitro* and *in vivo* was inversely related to endothelial cell proliferation these data strongly suggest that this protein may mediate the anti-proliferative effect of IC on these cells.

Fig. 2. IC-induced GBP-1 expression is inversely related to endothelial cell proliferation. (**A**) Western blot analyses of GBP-1 expression in HUVEC and MVEC treated as described in Figure 1(A), (**B**) after the addition of IL-1β (200 U/ml), TNF-α (300 U/ml) and IFN-γ (100 U/ml) alone or in the presence of AGF (VEGF and bFGF, 10 ng/ml each; corresponding signal intensities were densitometrically determined, lower panels) and (**C**) after the addition of IL-1β (20 U/ml), TNF-α (300 U/ml) or IFN-γ (100 U/ml) to HUVEC that were pre-incubated overnight (O.N.) in the presence or absence of AGF. (**D**) Northern blot and (**E**) western blot analyses of GBP-1 expression in MVEC after the addition of AGF or IL-1β (20 U/ml), alone or combined. Recombinant His$_6$-tagged GBP-1 was used as a protein standard for quantification. Corresponding signal intensities were densitometrically determined (lower panels, white columns) and compared with the proliferative capacity of MVEC under the same conditions (lower panels, black columns). Ethidium bromide (EtBr) visualization of blotted RNA, actin control (Actin). Northern blot analyses were carried out 5 h and western blot analyses 24 h after stimulation of the cells. A monoclonal rat anti-GBP-1 antibody was used for the detection of GBP-1.

GBP-1 mediates the IC-induced inhibition of endothelial cell proliferation

To determine whether GBP-1 mediates the anti-proliferative effect of IC, HUVEC were transduced with retroviral vectors that express a GBP-1 full-length cDNA in sense (Figure 5A, S) or antisense (Figure 5A, AS) orientation or with the control vector (Figure 5A, CR). In a long-term growth experiment similar proliferation rates were observed with CR- and AS-GBP-1-transduced cells (seven cell passages at a 1:4 splitting ratio after 3 months of culture in the presence of puromycin), whereas S-GBP-1-transduced cells grew significantly less (three cell passages for the same period of time), indicating that GBP-1 inhibits cell growth.

For a detailed analysis of cell growth under different conditions of stimulation, a short-term selection procedure (10 days) was used (see Materials and methods). After this time, GBP-1 protein synthesis was increased in IL-1β-treated control cells (Figure 5B, CR), but not in IL-1β-treated AS-GBP-1-expressing cells (Figure 5B, AS), demonstrating that expression of the endogenous GBP-1 gene was not impaired by the transduction procedure and that induction of the cellular GBP-1 protein was efficiently inhibited by the GBP-1 antisense RNA. HUVEC transduced with S-GBP-1 synthesized high levels of GBP-1 protein irrespective of the cell stimulation (Figure 5B, S).

Proliferation of HUVEC transduced with the control vector was stimulated in a dose-dependent manner by increasing the concentration of AGF (Figure 5C, gray bars). Under the same conditions AGF-stimulated proliferation of S-GBP-1-transduced cells was significantly lower (Figure 5C, white bars). On the other hand, AGF-induced proliferation of CR-transduced HUVEC was inhibited by IL-1β in a dose-dependent manner (Figure 5D, gray bars), whereas proliferation of AS-GBP-1-expressing cells was significantly higher especially in the presence of high IC concentrations (Figure 5D, black bars). Similar results were obtained with IFN-γ at concentrations of 10 up to 1000 U/ml (data not shown).

GBP-1 selectively inhibited cell proliferation, whereas IL-1β-induced adhesiveness for monocytes was unchanged in S-GBP-1-, AS-GBP-1- or CR-transduced HUVEC (Figure 5E). In addition, constitutive expression of GBP-1 in S-GBP-1-transduced cells did not impair the activation of the extracellular signal-regulated kinase (ERK)-1/2, a central MAP kinase, which is activated via
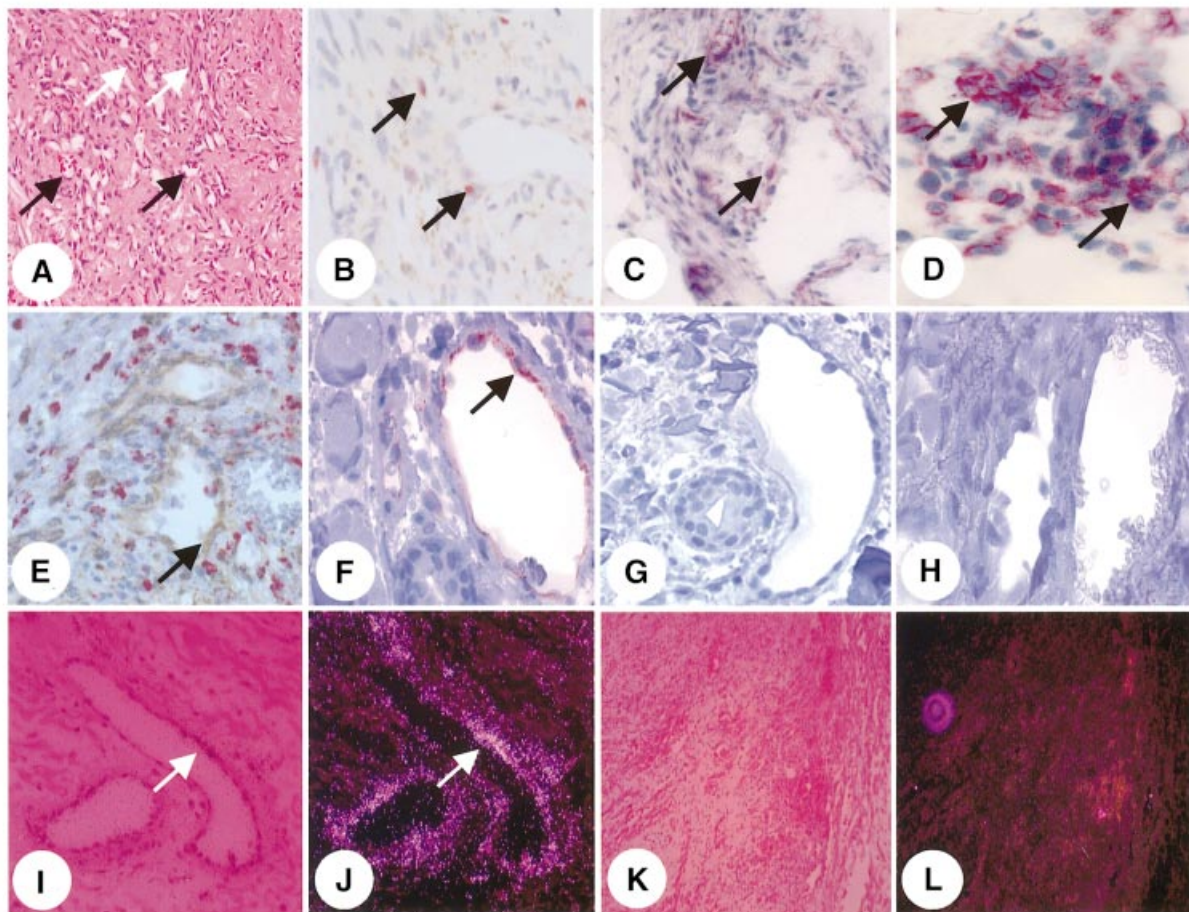

Fig. 3. GBP-1 is expressed in vessel endothelial cells of KS. (**A–D**) Staining of KS tissue sections by hematoxylin–eosin [A, blood vessels (black arrows), KS spindle cells (white arrows)] and by immunohistochemistry for detection of IL-1β (B, arrow), TNF-α (C, arrow) and IFN-γ (D, arrow). (**E**) Simultaneous staining of GBP-1 (brown, arrow) and the monocytic marker protein CD68 (red). (**F–H**) Immunodetection of GBP-1 in endothelial cells (F, arrow) and control staining of consecutive sections in the absence of the anti-GBP-1 antibody (G) or in the presence of a 320-fold molar

the Ras-Raf-MEK pathway in response to mitogenic stimulation (Figure 5F). Furthermore, TUNEL (TdT-mediated dUTP nick end labeling) analyses of apoptosis-associated nuclear DNA fragmentation (Figure 5G) and

western blot analyses of activation of the apoptotic initiator caspase 8 and the executioner caspase 3 (data not shown) yielded negative results in S-GBP-1-, AS-GBP-1- and CR-transduced cells, irrespective of their
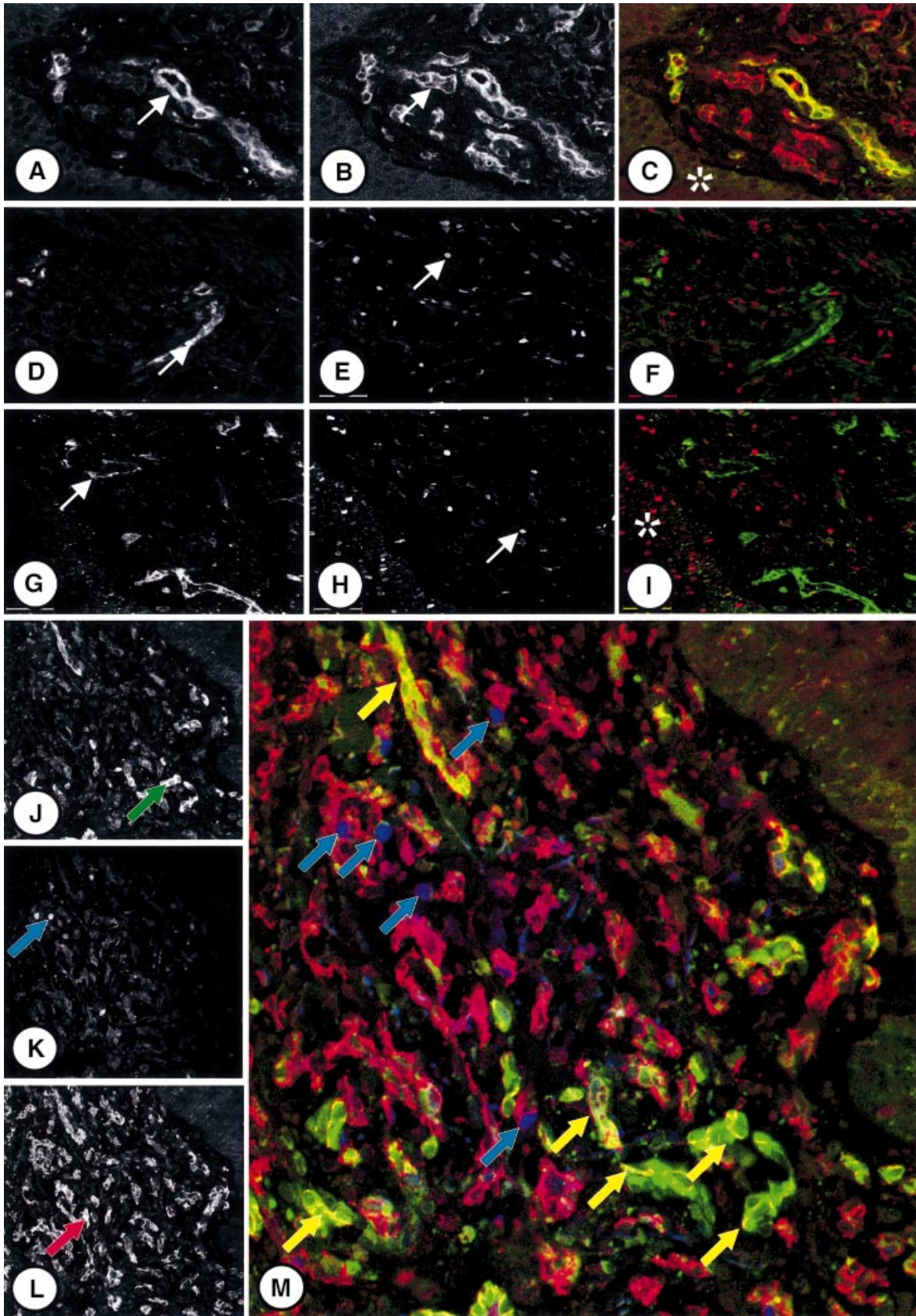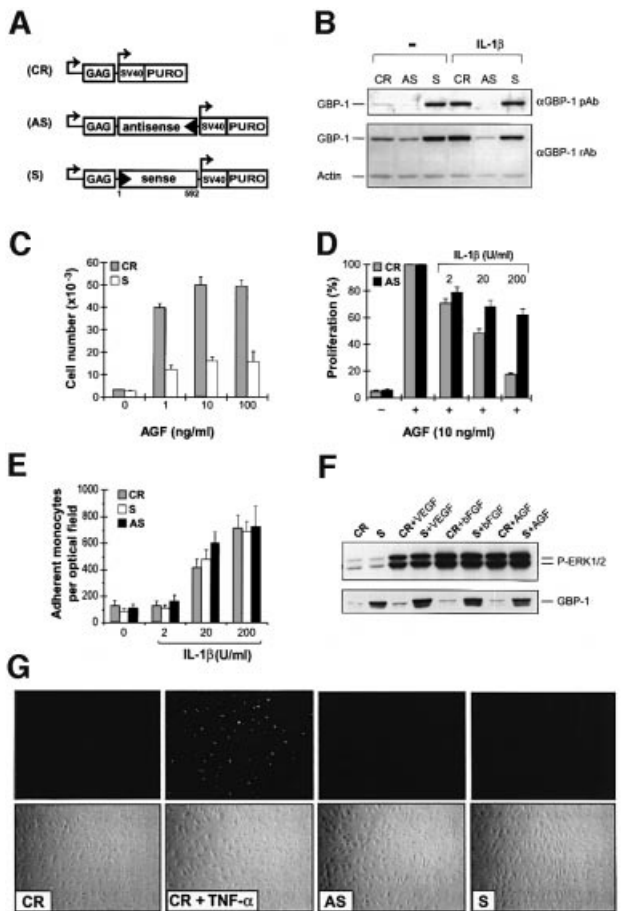
Fig. 5. GBP-1 mediates the inhibition of endothelial cell proliferation in response to IC. (**A**) Schematic presentation of the retroviral expression vector pBabePuro (control, CR) containing the full-length GBP-1 cDNA in sense (S-GBP-1, S) or antisense (AS-GBP-1, AS) orientation. (**B**) Western blot analysis of GBP-1 expression. Polyclonal rabbit anti-GBP-1 peptide antibody (αGBP-1 pAb), polyclonal rabbit anti-GBP-1 antibody (αGBP-1 rAb), actin control (Actin). After transduction, HUVEC were grown for 10 days in 0.3 µg/ml puromycin and then incubated for 24 h in the presence or absence of IL-1β (20 U/ml). (**C**) Proliferation experiments with S-GBP-1- (white columns) and CR- (gray columns) transduced HUVEC in the presence of increasing concentrations of AGF, and (**D**) with AS-GBP-1- (black columns) and CR- (gray columns) transduced HUVEC in the presence of AGF and increasing concentrations of IL-1β. (**E**) *In vitro* adhesion assay with S-GBP-1-, AS-GBP-1- and CR-transduced HUVEC stimulated with increasing concentrations of IL-1β and U937 monocytes. In (C), (D) and (E) the mean values obtained in three different transduction experiments are shown. (**F**) Western blot analyses of phospho-ERK-1/2 (upper panel) and GBP-1 (lower panel) expression in S-GBP-1- and CR-transduced HUVEC stimulated with either VEGF (10 ng/ml), bFGF (10 ng/ml) or AGF (VEGF and bFGF, 10 ng/ml each) for 15 min, respectively. (**G**) TUNEL analyses (upper panels) and the respective phase contrast images (lower panels) of untreated S-GBP-1-, AS-GBP-1- and CR-transduced HUVEC and as a positive control of apoptotic CR-transduced HUVEC incubated for 24 h in the presence of TNF-α (30 U/ml).

GBP-1 expression level. These results demonstrated that GBP-1 selectively inhibits cell proliferation and that this is not due to the inhibition of ERK-1/2 activation and occurs in the absence of apoptosis.

The helical domain of GBP-1 is sufficient to inhibit endothelial cell proliferation

Structural hallmarks of GBP-1 are a large globular α/β-domain harboring the GTPase activity, an elongated C-terminal part organized in an α-helical structure with unique features and a CaaX motif at the C-terminal end that causes isoprenylation of GBP-1 (Nantais *et al*., 1996; Prakash *et al*., 2000a,b). In order to identify the structural or functional component of the GBP-1 molecule responsible for the inhibition of endothelial cell proliferation, various mutants of the GBP-1 protein were generated (Figure 6A). First, the aspartate residue of the GTPase active site located at position +184 in the N-terminal globular domain of GBP-1 was mutated to an asparagine residue (Figure 6A, D184N). This mutation, in agreement with a previous report (Praefcke *et al*., 1999), abolished the GTPase activity of the molecule (Figure 6B, insert). Secondly, a TAA stop codon was introduced directly upstream of the sequences encoding the isoprenylation motif at the C-terminus of GBP-1 to block isoprenylation of the protein (Figure 6A, ΔCaaX). Thirdly, the cDNA fragments encoding the N-terminal globular domain (amino acids 1–290), which fully retains GTPase activity (C.Herrmann and G.Praefcke, personal communication) and the C-terminal helical domain (amino acids 288–592) were cloned separately into a retroviral vector (Figure 6A, Glo, Hel). Transduction of HUVEC with these constructs
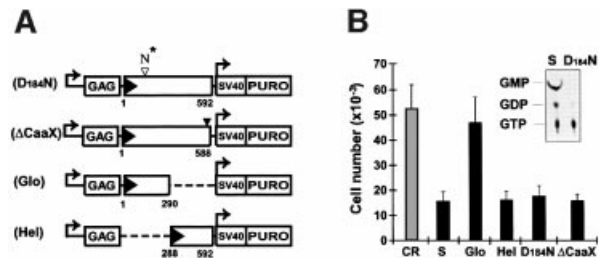

Fig. 6. The helical domain of GBP-1 is sufficient to inhibit endothelial cell proliferation. (**A**) Schematic presentation of the retroviral expression vector pBabePuro encoding various mutants of GBP-1: GTPase-deficient (D184N-GBP-1, D184N) and isoprenylation motif-deleted (ΔCaaX-GBP-1, ΔCaaX) GBP-1, separated N-terminal globular domain (Glo-GBP-1, Glo) and C-terminal helical domain (Hel-GBP-1, Hel). The numbers refer to the positions of the amino acids in GBP-1. The D to N mutation in the GTPase motif is indicated by an open triangle and the black triangle indicates the TAA stop codon inserted upstream of the encoded CaaX motif. (**B**) Proliferation experiments with transduced HUVEC in the presence of AGF (10 ng/ml) and GTPase assay of purified wild-type GBP-1 and D184N-GBP-1 (insert).

Fig. 4. GBP-1 expression correlates inversely with endothelial cell proliferation in KS. (**A–C**) Immunofluorescence staining of KS tissue sections for the detection of GBP-1 and CD31 antigens. Detection of GBP-1 (A, arrow), CD31 (B, arrow) alone and in combination (C, GBP-1, green cytoplasmic staining; CD31, red cytoplasmic staining, colocalization yellow). The epidermal layer overlaying the lesions is indicated by an asterisk. (**D–I**) Detection of GBP-1 (D and G, arrows) and Ki67 (E and H, arrows) alone and in combination (F and I, GBP-1, green, Ki67, red nuclear staining) in different KS specimens. Ki67 positive basal cells in the epidermis are labeled by an asterisk. (**J–M**) Triple labeling experiment for the detection of GBP-1 (J, green arrow), Ki67 (K, blue arrow) and CD31 (L, red arrow) alone or in combination (M, CD31, red; GBP-1, green; Ki67, blue). Ki67/CD31 (blue arrows) and GBP-1/CD31 (yellow arrows) double-positive endothelial cells are indicated.

and determination of the proliferative capability of these cells in the presence of AGF revealed that expression of the globular domain did not inhibit proliferation, whereas the C-terminal helical domain as well as the D184N and ΔCaaX mutants had similar inhibitory activity to wild-type GBP-1 (Figure 6B). This demonstrated that the anti-proliferative effect of GBP-1 is not dependent on the GTPase activity or the isoprenylation motif of the molecule but is specifically mediated by its helical domain.

Discussion

GBP-1 is among the major IFN-γ-induced factors and belongs to the group of large GTP-binding proteins that includes Mx proteins and dynamin (Prakash *et al.*, 2000a). It is characterized by a high-turnover GTPase activity (van der Bliek, 1999; Prakash *et al.*, 2000a) and has been shown to mediate antiviral effects against the vesicular stomatitis virus and the encephalomyocarditis virus in HeLa cells (Anderson *et al.*, 1999). In this study we showed that GBP-1 is a key mediator of the anti-proliferative effect of IC on endothelial cells and a molecular marker of the IC-activated non-proliferating phenotype of endothelial cells *in vitro* and *in vivo*.

GBP-1 was identified by DDRT–PCR to be expressed in endothelial cells stimulated with IL-1β, TNF-α or IFN-γ, but not in AGF-stimulated or unstimulated cells. Since the same IC are also potent inhibitors of AGF-induced endothelial cell proliferation, this suggested that GBP-1 expression may characterize the non-proliferating phenotype of endothelial cells that is induced by IC. We confirmed this hypothesis by demonstrating that the expression of GBP-1 induced by IC correlated inversely with endothelial cell proliferation and was inhibited by AGF in both microvascular and macrovascular endothelial cells (Figure 2).

Although IFN-γ can induce *in vitro* expression of GBP-1 in several different cell types including monocytes/macrophages, fibroblasts and keratinocytes (Bandyopadhyay *et al.*, 1992; Shuai *et al.*, 1992; Saunders *et al.*, 1999), in KS tissues GBP-1 expression was almost exclusively detected in vessel endothelial cells but not in the KS spindle cells, monocytes/macrophages, lymphocytes, fibrocytes of the dermis or in the keratinocytes of the epidermis (Figure 4), suggesting that GBP-1 expression *in vivo* is more closely associated with vessel endothelial cells as compared with cultivated cells *in vitro*.

As was observed *in vitro*, GBP-1 expression was selectively associated with the IC-activated non-proliferating phenotype of endothelial cells also *in vivo*. In fact, in KS lesions GBP-1 expression was only detected in non-proliferating endothelial cells (CD31-positive, Ki67-negative) of vessels that were surrounded by numerous infiltrating monocytes and lymphocytes, which produced IC (Figure 3) (Stürzl *et al.*, 1995; Fiorelli *et al.*, 1998). By contrast, GBP-1 was never detected in proliferating endothelial cells (CD31-positive, Ki67-positive) that are stimulated by the bFGF and VEGF released from the KS spindle cells (Xerri *et al.*, 1991; Ensoli *et al.*, 1994; Cornali *et al.*, 1996). In KS tumor areas characterized by numerous KS spindle cells and little inflammatory cell infiltration,

GBP-1 expression was generally restricted to a few non-proliferating endothelial cells in areas with high concentrations of IC. These results define GBP-1 as a novel marker of the IC-induced non-proliferative phenotype of endothelial cells *in vitro* and *in vivo*.

The close association of GBP-1 expression with the non-proliferating phenotype induced by IC on endothelial cells *in vitro* and *in vivo* suggested that GBP-1 is an inhibitor of endothelial cell proliferation. In fact, experiments with retrovirally transduced endothelial cells demonstrated that the constitutive expression of GBP-1 inhibits cell proliferation, whereas the inhibition of endogenous GBP-1 expression abrogates the anti-proliferative effect of IC (Figure 5). Therefore, GBP-1 is a major mediator of the anti-proliferative effect of IC on endothelial cells. Notably, GBP-1 inhibits cell proliferation in the absence of apoptosis, suggesting that the GBP-1-mediated inhibition of cell proliferation may be reversible.

The structure–function analysis of the GBP-1 molecule demonstrated that the isoprenylation of the protein at the C-terminal end as well as the GTPase activity and the whole globular domain encoding this activity are not required for inhibition of cell proliferation (Figure 6). In contrast, expression of the C-terminal helical domain inhibited AGF-induced proliferation to a similar extent to wild-type GBP-1. This indicated that the helical domain is the mediator of the GBP-1 anti-proliferative activity.

Neither constitutive expression of GBP-1 nor the inhibition of cellular GBP-1 synthesis affected the IC-induced adhesiveness for monocytes of transduced endothelial cells. This is in agreement with data showing that VEGF, similarly to IC, induces adhesiveness of endothelial cells *in vitro* (Melder *et al.*, 1996; Lu *et al.*, 1999; Kim *et al.*, 2001) and *in vivo* (Detmar *et al.*, 1998) but has opposite effects on cell proliferation. Both findings clearly suggest that adhesiveness and proliferation are independently regulated cellular responses of endothelial cells.

The independent regulation of the IC-induced anti-proliferative response and cell adhesiveness may open new avenues for the therapeutic use of GBP-1 or its active domain as an anti-angiogenic molecule. On the other hand, inhibition of GBP-1 expression may restore vessel proliferative activity under inflammatory conditions, for example to support collateral vessel formation. In addition, GBP-1 expression may be used as a molecular marker of IC-activated endothelial cells. Thus, GBP-1 may provide an important tool and target to dissect the complex activity of IC on endothelial cells, and to detect and specifically modulate the IC-induced non-proliferating phenotype of endothelial cells in vascular diseases.

Notably, the major activation pathways of endothelial cells, namely the IC pathway and the AGF pathway, converge in the regulation of GBP-1 expression. Thus, the natural function of GBP-1 in tissues may be the induction of a transient potentially reversible non-proliferating endothelial cell phenotype as a dose-integrated response to a microenvironment with relatively increased IC concentrations.

Materials and methods

Cell cultures

HUVEC and MVEC were maintained in endothelial cell basal medium (EBM, Clonetics) supplemented with 5% fetal bovine serum (FBS). The U937 monocytic cell line was grown in RPMI 1640–10% FBS. Before stimulation, cells were cultured overnight in EBM–0.5% FBS. Recombinant human VEGF165 was purchased from R&D Systems, recombinant human bFGF, IL-1β, IFN-γ and TNF-α from Roche.

Cell proliferation assays. Cells were seeded into 24-well plates in EBM–0.5% FBS at 10^3 cells/cm^2 (HUVEC) or 0.5×10^3 cells/cm^2 (MVEC), respectively. Cytokines and/or growth factors were added every second day. After 6 days cell numbers were determined with a Coulter counter (Coulter Electronics). Each experiment was carried out in triplicate and the results expressed as the mean of cell numbers ($\pm$ SD).

Cell adhesion assays. Transduced HUVEC were seeded at 7×10^4 cells/cm^2 in eight-well microchamber slides (Nunc) and incubated overnight in EBM–2.5% FBS. Cytokines were added in EBM–0.5% FBS for 6 h at concentrations indicated in the figures. Subsequently, 500 µl of a suspension of U937 cells (5×10^5 cells/ml) were added, and after 15 min non-adherent monocytes were gently removed by dipping the slides into RPMI 1640–1% FBS. Afterwards, the cells were fixed (30 min, RPMI 1640–1% FBS–5% glutaraldehyde) and the adherent U937 cells were counted using a photo-imaging system (Optimas, Stemmer Electronics). Each experiment was carried out in triplicate and the results expressed as the mean of adherent cells in 10 different optical fields/well ($\pm$ SD).

DDRT–PCR

The RNAimage kit (GenHunter Corporation) was used for this procedure according to the manufacturer's instructions.

Retroviral vectors

The cDNA encoding full-length human GBP-1 (GBP-1 cDNA) was generated by RT–PCR using total cellular RNA isolated from IFN-γ/IL-1β-treated (100 U/ml, 20 U/ml, 5 h) MVEC. cDNA fragments encoding the helical (Hel-cDNA) or globular (Glo-cDNA) domain were synthesized by PCR using the amplified GBP-1 cDNA as a template. cDNA fragments were cloned into the Moloney murine leukemia virus-derived retroviral vector pBabePuro (Morgenstern and Land, 1990). All PCR primers encoded a unique restriction site (underlined). In addition, an optimal Kozak consensus sequence (italic) was introduced in front of the ATG start codon (bold) in all 5′ primers. Sequences of 5′ primers: GBP-1 cDNA and Glo-cDNA, 5′-CCG<u>GAATTC</u>*GCCGCC***ATG**GCAT-CAGAGATCCACATG-3′ [positions +69 to +89, for reference see sequence of human GBP-1 mRNA (Cheng *et al.*, 1991)]; Hel-cDNA, 5′-CCG<u>GAATTC</u>*GCCGCC***ATG**GTCAACGGGCCTCGTCT-AGAG-3′ (+930 to +950). Sequences of 3′ primers: GBP-1 cDNA and Hel-cDNA, 5′-CGC<u>GGATCCGAATTC</u>TTAGCTTATGGTACATGC-CTTTCG-3′ (+1824 to +1847); Glo-cDNA, 5′-CGC<u>GGATCCGAATTC</u>-TTACCCGTTGACCTGGATGCC-3′ (+938 to +921).

The mutant D184N- and ΔCaaX-cDNAs were generated by site-directed mutagenesis (QuickChange kit, Stratagene). In the D184N-cDNA a G to A transition was introduced at position +618 and in the ΔCaaX-cDNA a 5′-TAA-3′ stop codon was introduced at position +1833. Identity of all cDNA molecules was confirmed by sequence analysis.

Transduction of HUVEC

The packaging cell line PG13/J7 (Miller *et al.*, 1991) was cultured in DMEM–10% FBS–1× HAT supplement (Life technologies) and transfected with 5 µg of purified plasmid DNA using Superfect (Qiagen). Stably transfected cell lines were established by cultivation in the presence of 3 µg/ml puromycin (Sigma). Recombinant viruses were obtained from these cells at 80% confluence, by adding fresh DMEM–10% FBS without puromycin for 12 h. Cell culture supernatants were harvested and filtered (0.45 µm, Millipore). Titers of retroviral particles in the cell supernatants were compared by subjecting isolated viral RNA to two different endpoint titration approaches of semi-quantitative RT–PCR using primer pairs binding specifically to the viral genomic RNA. Isolated viral RNA was either serially diluted and subjected to 35 amplification cycles, or diluted 1:40 and subjected to increasing numbers (25, 30, 35, 40) of PCR cycles.

Retroviral infection of HUVEC was carried out by incubating the cells twice (4 h each) with titer-adjusted virus in the presence of polybrene (final concentration 8 µg/ml). Between the two infection steps, the cells were kept for 4 h in EBM–5% FBS. Under these conditions transduction efficiency was 50%, as determined by immunochemical detection of GBP-1 at the single-cell level. Forty-eight hours after infection, 0.3 µg/ml of puromycin was added and transduced cells were cultured for an additional 10 days (short-term selection procedure) and used for proliferation experiments.

For the long-term proliferation experiments, 1×10^4 transduced HUVEC were seeded into Petri dishes (3 cm diameter) in EBM–5% FBS containing puromycin (0.3 µg/ml), grown to confluence and split in a 1:4 ratio. This was defined as one passage.

Purification of His₆-tagged GBP-1

His$_6$-tagged GBP-1 and D184N-GBP-1 were produced in *Escherichia coli* M15 and purified by standard Ni-NTA–agarose column chromatography (Qiagen).

Antibody production

Anti-GBP-1 antibodies were generated by using either affinity-purified His$_6$-tagged GBP-1 (polyclonal rabbit anti-GBP-1 antibody, monoclonal rat anti-GBP-1 antibody) or a peptide with the 21 C-terminal amino acids (MKNEIQDLQTKMRRRKAYTIS) of GBP-1 (polyclonal rabbit anti-GBP-1 peptide antibody) by standard procedures.

GTPase assay

GTPase assays were carried out as described (Pitossi *et al.*, 1993) using 125 ng/µl purified His$_6$-tagged wild-type GBP-1 or D184N-GBP-1.

Northern blot and western blot analyses

Northern blot analysis was carried out with 25 µg of total cellular RNA as described (Cornali *et al.*, 1996). For western blot analysis the following antibodies diluted in 0.5× Western Blocking Reagent Solution (Roche) and 0.1% Tween 20 (Sigma) were used: polyclonal rabbit anti-GBP-1 antibody (1:5000), polyclonal rabbit anti-GBP-1 peptide antibody (1:250), rat monoclonal anti-GBP-1 antibody (1:500), polyclonal rabbit anti-actin antibody (1:2000), polyclonal rabbit anti-phospho-ERK-1/2 antibody (1:1000, New England Biolabs), mouse monoclonal anti-caspase 3 and anti-caspase 8 antibodies (1:350, Zymed).

RT–PCR analyses

The Titan one-tube RT–PCR system (Roche) was used for this procedure according to the manufacturer's instructions. Primers: IFN-γ, forward, 5′-GACCAGAGCATCCAAAAGAGTGTG-3′, reverse, 5′-AAGCACT-GGCTCAGATTGCAGG-3′ (644 bp fragment); actin, forward, 5′-CCA-AGGCCAACCGCGAGAAGATGAC-3′, reverse, 5′-AGGGTACATG-GTGGTGCCGCCAGAC-3′ (585 bp fragment).

TUNEL analyses

The *in situ* cell death detection kit, fluorescein (Roche), was used for this procedure according to the manufacturer's instructions. Transduced HUVEC subjected to this procedure were seeded at 10^4 cells/cm^2 in eight-well microchamber slides (Lab-Tec) and incubated overnight in EBM–0.5% FBS. Then cells were incubated for 24 h in EBM–5% FBS or EBM–0.5% FBS–30 U/ml TNF-α (positive control) and fixed in 100% EtOH (30 min, 4°C). Apoptotic cells were detected by fluorescence microscopy.

Tissue biopsies

Twelve KS biopsy specimens derived from skin lesions of human immunodeficiency virus (HIV)-1-infected homosexual male patients classified as Centers for Disease Control and Prevention group C were studied. Four control biopsy specimens were obtained from an uninvolved area of the skin of the patients. All biopsies were taken for diagnostic purposes after the informed consent of the patients. Immediately after excision, tissues were either cryopreserved (i.e. for detection of TNF-α and IFN-γ) or fixed in 4% paraformaldehyde and embedded in paraffin (for all other stainings).

In situ hybridization

In situ hybridization was carried out on paraffin-embedded tissue sections as described (Stürzl *et al.*, 1999). The plasmid pCR-Script SK(+) (Stratagene) containing the full-length GBP-1 cDNA was used for the synthesis of ^{35}S-radiolabeled sense and antisense RNA hybridization probes (sp. act. $\geqslant 1 \times 10^9$ c.p.m./µg RNA).

Immunostaining of cells

HUVEC were fixed in ethanol for 20 min at 4°C. The rat monoclonal anti-GBP-1 antibody (1:100) was used as primary antibody. For the detection reaction the ABC Elite kit (Linaris) and the 3,3′-diaminobenzidine (DAB) substrate (Biogenex) were used.

Immunostaining of tissue sections

Frozen sections. Specimens were fixed in cold acetone (–20°C) and stained by the alkaline phosphatase–anti-alkaline phosphatase (APAAP) method. Mouse monoclonal antibodies to IFN-γ (1:25, Genzyme Diagnostics) and TNF-α (1:200, Dako) were used as described previously (Fiorelli *et al.*, 1998).

Paraffin sections. Sections were microwave-treated (three times, 10 min, 580 W) in Target Retrieval Solution pH 9.0 (Dako). The monoclonal rat anti-GBP-1 antibody (1:300 in dilution medium, Dako) and a monoclonal mouse anti-IL-1β antibody (1:10, Dianova) were used as primary antibodies. For the detection reactions either the ABC Elite kit and the AEC substrate or an APAAP staining kit and the Fast Red substrate were used according to the manufacturers' instructions.

For simultaneous detection of GBP-1 and CD68, DAB was used as a substrate in the peroxidase reaction for detection of GBP-1. Subsequently, sections were washed twice for 5 min in Tris (0.05 M, pH 7.4/Brij 0.5%), incubated with a monoconal mouse anti-CD68 antibody (1:200, Dako) and subsequently with a rabbit anti-mouse IgG antibody (1:25, Dako) and the APAAP (mouse) complex (Dako). VectorRed (Linaris) was used as a substrate for the color reaction.

After the immunohistochemical procedure, sections were counterstained with hematoxylin and mounted with Immunomount (Shandon).

Fluorescence staining

Double staining. For double staining of GBP-1 and Ki67 or CD31, tissue sections were microwave-treated (three times, 10 min, 580 W) either in Enhancer Receptor buffer (Linaris) for detection of GBP-1/Ki67 or in Target Retrieval Solution pH 9.0 (Dako) for GBP-1/CD31 detection. The slides were then incubated with a mixture of rat anti-GBP-1 (1:20)/mouse anti-CD31 (1:20, Serotec) or rat anti-GBP-1 (1:20)/mouse anti-Ki67 (1:20, Dako) monoclonal antibodies, respectively. Bound primary antibodies were detected with a mixture of highly cross-absorbed goat anti-rat and goat anti-mouse antibodies (1:500) coupled to the fluorochromes AlexaFluor488 and AlexaFluor546 (Molecular Probes Europe), respectively.

Triple staining. For triple staining of GBP-1, CD31 and Ki67 sections were initially treated as described above for GBP-1/CD31 double staining and than successively incubated with 10% normal mouse serum and goat Fab anti-mouse fragments 1:20 (Dianova), for 40 min each. Afterwards, the slides were incubated with the anti-Ki67 antibody (1:20) and, finally, with a highly cross-absorbed goat anti-mouse antibody (1:500) coupled to the AlexaFluor350 fluorochrome.

For visualization of bound fluorochromes, slides were mounted in PBS and examined using a Zeiss light scanning confocal microscope.

Acknowledgements

References

Anderson,S.L., Carton,J.M., Lou,J., Xing,L. and Rubin,B.Y. (1999) Interferon-induced guanylate binding protein-1 (GBP-1) mediates an antiviral effect against vesicular stomatitis virus and encephalomyocarditis virus. *Virology*, **256**, 8–14.

Bandyopadhyay,S.K., Kumar,R., Rubin,B.Y. and Sen,G.C. (1992) Interferon-inducible gene expression in HL-60 cells: effects of the state of differentiation. *Cell Growth Differ.*, **3**, 369–375.

Bevilacqua,M.P., Pober,J.S., Wheeler,M.E., Cotran,R.S. and Gimbrone,M.A.,Jr (1985) Interleukin 1 acts on cultured human vascular endothelium to increase the adhesion of polymorphonuclear leukocytes, monocytes, and related leukocyte cell lines. *J. Clin. Invest.*, **76**, 2003–2011.

Carmeliet,P. and Jain,R.K. (2000) Angiogenesis in cancer and other diseases. *Nature*, **407**, 249–257.

Cavender,D.E., Edelbaum,D. and Welkovich,L. (1991) Effects of inflammatory cytokines and phorbol esters on the adhesion of U937 cells, a human monocyte-like cell line, to endothelial cell monolayers and extracellular matrix proteins. *J. Leukoc. Biol.*, **49**, 566–578.

Cheng,Y.S., Patterson,C.E. and Staeheli,P. (1991) Interferon-induced guanylate-binding proteins lack an N(T)KXD consensus motif and bind GMP in addition to GDP and GTP. *Mol. Cell. Biol.*, **11**, 4717–4725.

Cines,D.B. *et al.* (1998) Endothelial cells in physiology and in the pathophysiology of vascular disorders. *Blood*, **91**, 3527–3561.

Cornali,E., Zietz,C., Benelli,R., Weninger,W., Masiello,L., Breier,G., Tschachler,E., Albini,A. and Stürzl,M. (1996) Vascular endothelial growth factor regulates angiogenesis and vascular permeability in Kaposi's sarcoma. *Am. J. Pathol.*, **149**, 1851–1869.

Cozzolino,F., Torcia,M., Aldinucci,D., Ziche,M., Almerigogna,F., Bani,D. and Stern,D.M. (1990) Interleukin 1 is an autocrine regulator of human endothelial cell growth. *Proc. Natl Acad. Sci. USA*, **87**, 6487–6491.

Detmar,M. *et al.* (1998) Increased microvascular density and enhanced leukocyte rolling and adhesion in the skin of VEGF transgenic mice. *J. Invest. Dermatol.*, **111**, 1–6.

Ensoli,B. *et al.* (1994) Synergy between basic fibroblast growth factor and HIV-1 Tat protein in induction of Kaposi's sarcoma. *Nature*, **371**, 674–680.

Ensoli,B., Sgadari,C., Barillari,G., Sirianni,M.C., Stürzl,M. and Monini,P. (2001) Biology of Kaposi's sarcoma. *Eur. J. Cancer*, **37**, 1251–1269.

Fajardo,L.F., Kwan,H.H., Kowalski,J., Prionas,S.D. and Allison,A.C. (1992) Dual role of tumor necrosis factor-α in angiogenesis. *Am. J. Pathol.*, **140**, 539–544.

Fathallah-Shaykh,H.M., Zhao,L.J., Kafrouni,A.I., Smith,G.M. and Forman,J. (2000) Gene transfer of IFN-γ into established brain tumors represses growth by antiangiogenesis. *J. Immunol.*, **164**, 217–222.

Ferrara,N. and Henzel,W.J. (1989) Pituitary follicular cells secrete a novel heparin-binding growth factor specific for vascular endothelial cells. *Biochem. Biophys. Res. Commun.*, **161**, 851–858.

Fiorelli,V. *et al.* (1998) γ-Interferon produced by CD8+ T cells infiltrating Kaposi's sarcoma induces spindle cells with angiogenic phenotype and synergy with human immunodeficiency virus-1 Tat protein: an immune response to human herpesvirus-8 infection? *Blood*, **91**, 956–967.

Folkman,J. and Klagsbrun,M. (1987) Angiogenic factors. *Science*, **235**, 442–447.

Frater-Schroder,M., Risau,W., Hallmann,R., Gautschi,P. and Bohlen,P. (1987) Tumor necrosis factor type α, a potent inhibitor of endothelial cell growth *in vitro*, is angiogenic *in vivo*. *Proc. Natl Acad. Sci. USA*, **84**, 5277–5281.

Friesel,R., Komoriya,A. and Maciag,T. (1987) Inhibition of endothelial cell proliferation by γ-interferon. *J. Cell Biol.*, **104**, 689–696.

Gerol,M., Curry,L., McCarroll,L., Doctrow,S. and RayChaudhury,A. (1998) Growth regulation of cultured endothelial cells by inflammatory cytokines: mitogenic, anti-proliferative and cytotoxic effects. *Comp. Biochem. Physiol. C Pharmacol. Toxicol. Endocrinol.*, **120**, 397–404.

Griffioen,A.W., Damen,C.A., Blijham,G.H. and Groenewegen,G. (1996a) Tumor angiogenesis is accompanied by a decreased inflammatory response of tumor-associated endothelium. *Blood*, **88**, 667–673.

Griffioen,A.W., Damen,C.A., Martinotti,S., Blijham,G.H. and Groenewegen,G. (1996b) Endothelial intercellular adhesion molecule-1 expression is suppressed in human malignancies: the role of angiogenic factors. *Cancer Res.*, **56**, 1111–1117.

Joseph,I.B. and Isaacs,J.T. (1998) Macrophage role in the anti-prostate cancer response to one class of antiangiogenic agents. *J. Natl Cancer Inst.*, **90**, 1648–1653.

Keck,P.J., Hauser,S.D., Krivi,G., Sanzo,K., Warren,T., Feder,J. and

Connolly,D.T. (1989) Vascular permeability factor, an endothelial cell mitogen related to PDGF. *Science*, **246**, 1309–1312.

Kim,I., Moon,S.O., Kim,S.H., Kim,H.J., Koh,Y.S. and Koh,G.Y. (2001) VEGF stimulates expression of ICAM-1, VCAM-1 and E-selectin through nuclear factor-κB activation in endothelial cells. *J. Biol. Chem.*, **276**, 7614–7620.

Liang,P. and Pardee,A.B. (1992) Differential display of eukaryotic messenger RNA by means of the polymerase chain reaction. *Science*, **257**, 967–971.

Lu,M., Perez,V.L., Ma,N., Miyamoto,K., Peng,H.B., Liao,J.K. and Adamis,A.P. (1999) VEGF increases retinal vascular ICAM-1 expression *in vivo*. *Invest. Ophthalmol. Vis. Sci.*, **40**, 1808–1812.

Mahadevan,V., Hart,I.R. and Lewis,G.P. (1989) Factors influencing blood supply in wound granuloma quantitated by a new *in vivo* technique. *Cancer Res.*, **49**, 415–419.

Melder,R.J., Koenig,G.C., Witwer,B.P., Safabakhsh,N., Munn,L.L. and Jain,R.K. (1996) During angiogenesis, vascular endothelial growth factor and basic fibroblast growth factor regulate natural killer cell adhesion to tumor endothelium. *Nature Med.*, **2**, 992–997.

Miller,A.D., Garcia,J.V., von Suhr,N., Lynch,C.M., Wilson,C. and Eiden,M.V. (1991) Construction and properties of retrovirus packaging cells based on gibbon ape leukemia virus. *J. Virol.*, **65**, 2220–2224.

Montrucchio,G., Lupia,E., Battaglia,E., Passerini,G., Bussolino,F., Emanuelli,G. and Camussi,G. (1994) Tumor necrosis factor α-induced angiogenesis depends on *in situ* platelet-activating factor biosynthesis. *J. Exp. Med.*, **180**, 377–382.

Morgenstern,J.P. and Land,H. (1990) Advanced mammalian gene transfer: high titre retroviral vectors with multiple drug selection markers and a complementary helper-free packaging cell line. *Nucleic Acids Res.*, **18**, 3587–3596.

Nantais,D.E., Schwemmle,M., Stickney,J.T., Vestal,D.J. and Buss,J.E. (1996) Prenylation of an interferon-γ-induced GTP-binding protein: the human guanylate binding protein, huGBP1. *J. Leukoc. Biol.*, **60**, 423–431.

Norioka,K., Mitaka,T., Mochizuki,Y., Hara,M., Kawagoe,M. and Nakamura,H. (1994) Interaction of interleukin-1 and interferon-γ on fibroblast growth factor-induced angiogenesis. *Jpn J. Cancer Res.*, **85**, 522–529.

Pitossi,F., Blank,A., Schroder,A., Schwarz,A., Hussi,P., Schwemmle,M., Pavlovic,J. and Staeheli,P. (1993) A functional GTP-binding motif is necessary for antiviral activity of Mx proteins. *J. Virol.*, **67**, 6726–6732.

Praefcke,G.J., Geyer,M., Schwemmle,M., Robert Kalbitzer,H. and Herrmann,C. (1999) Nucleotide-binding characteristics of human guanylate-binding protein 1 (hGBP1) and identification of the third GTP-binding motif. *J. Mol. Biol.*, **292**, 321–332.

Prakash,B., Praefcke,G.J., Renault,L., Wittinghofer,A. and Herrmann,C. (2000a) Structure of human guanylate-binding protein 1 representing a unique class of GTP-binding proteins. *Nature*, **403**, 567–571.

Prakash,B., Renault,L., Praefcke,G.J., Herrmann,C. and Wittinghofer,A. (2000b) Triphosphate structure of guanylate-binding protein 1 and implications for nucleotide binding and GTPase mechanism. *EMBO J.*, **19**, 4555–4564.

Samaniego,F., Markham,P.D., Gendelman,R., Gallo,R.C. and Ensoli,B. (1997) Inflammatory cytokines induce endothelial cells to produce and release basic fibroblast growth factor and to promote Kaposi's sarcoma-like lesions in nude mice. *J. Immunol.*, **158**, 1887–1894.

Saunders,N.A., Smith,R.J. and Jetten,A.M. (1999) Regulation of guanylate-binding protein expression in interferon-γ-treated human epidermal keratinocytes and squamous cell carcinoma cells. *J. Invest. Dermatol.*, **112**, 977–983.

Schweigerer,L., Malerstein,B. and Gospodarowicz,D. (1987) Tumor necrosis factor inhibits the proliferation of cultured capillary endothelial cells. *Biochem. Biophys. Res. Commun.*, **143**, 997–1004.

Shuai,K., Schindler,C., Prezioso,V.R. and Darnell,J.E., Jr (1992) Activation of transcription by IFN-γ: tyrosine phosphorylation of a 91-kD DNA binding protein. *Science*, **258**, 1808–1812.

Stürzl,M., Brandstetter,H., Zietz,C., Eisenburg,B., Raivich,G., Gearing,D.P., Brockmeyer,N.H. and Hofschneider,P.H. (1995) Identification of interleukin-1 and platelet-derived growth factor-B as major mitogens for the spindle cells of Kaposi's sarcoma: a combined *in vitro* and *in vivo* analysis. *Oncogene*, **10**, 2007–2016.

Stürzl,M. *et al.* (1999) Expression of K13/v-FLIP gene of human herpesvirus 8 and apoptosis in Kaposi's sarcoma spindle cells. *J. Natl Cancer Inst.*, **91**, 1725–1733.

Stürzl,M., Zietz,C., Monini,P. and Ensoli,B. (2001) Human herpes-virus-8 and Kaposi's sarcoma: relationship with the multistep concept of tumorigenesis. *Adv. Cancer Res.*, **81**, 125–159.

Torisu,H., Ono,M., Kiryu,H., Furue,M., Ohmoto,Y., Nakayama,J., Nishioka,Y., Sone,S. and Kuwano,M. (2000) Macrophage infiltration correlates with tumor stage and angiogenesis in human malignant melanoma: possible involvement of TNFα and IL-1α. *Int. J. Cancer*, **85**, 182–188.

van der Bliek,A.M. (1999) Functional diversity in the dynamin family. *Trends Cell Biol.*, **9**, 96–102.

Xerri,L., Hassoun,J., Planche,J., Guigou,V., Grob,J.J., Parc,P., Birnbaum,D. and deLapeyriere,O. (1991) Fibroblast growth factor gene expression in AIDS-Kaposi's sarcoma detected by *in situ* hybridization. *Am. J. Pathol.*, **138**, 9–15.

Yilmaz,A., Bieler,G., Spertini,O., Lejeune,F.J. and Ruegg,C. (1998) Pulse treatment of human vascular endothelial cells with high doses of tumor necrosis factor and interferon-γ results in simultaneous synergistic and reversible effects on proliferation and morphology. *Int. J. Cancer*, **77**, 592–599.